# 論文 / 著書情報
# Article / Book Information

| | |
|---|---|
| Title(English) | Full-Scale CFD Simulation of Microchannel Heat Exchanger with S-Shaped Fins |
| Authors(English) | Motoaki Utamura, Nikitin Konstantin |
| Citation(English) | The 19th Intn ’ l. Symposium on Transport Phenomena(ISTP2008), paper No.129 |
| 発行日 / Pub. date | 2008, |

# FULL-SCALE CFD SIMULATION OF MICHROCHANNEL HEAT EXCHANGER WITH S-SHAPED FINS

*M. Utamura* [1], *K. Nikitin* [2]
[1]Tokyo Institute of Technology,Tokyo, JAPAN
[2]Paul Scherrer Institut, Villigen PSI, SWITZERLAND

## ABSTRACT

Heat transfer and pressure drop characteristics of michrochannel heat exchanger (MCHE) with fluid channels formed by S-shaped fins have been calculated by CFD code FLUENT. Three central plates or ¼ part of heat exchanger have been simulated. The simulation results are compared with the previously obtained experimental data. The FLUENT code satisfactory predicts the main thermo-hydraulic characteristics of MCHE. The heat transfer rate and pressure drop is approximately 1.5 times less in the inlet/outlet distributors comparing to those in the cross-flow parts of MCHE.

## INTRODUCTION

A Micro-Channel Heat Exchanger (MCHE) is considered to be a promising candidate as a recuperator of a high-temperature gas-cooled reactor. Particularly, MCHEs were applied as low-temperature and high-temperature recuperators for gas-turbine CO2 cycle [1, 2](Kato, 2004; Muto, 2003). A new MCHE, with S-shaped fins based on a sine curve, was proposed in a previous study [3] (Tsuzuki, 2005). This heat exchanger incorporates non-continuous sine-like zigzag fluid channels that are chemically etched into metal plates. The plates are then diffusion-bonded under high-pressure and high-temperature conditions to form a heat exchanger core of required capacity. Because of diffusion bonding technology, the MCHE possesses the parent material strength.

The heat transfer and pressure drop characteristics of MCHE with S-shaped fins have been studied experimentally [4] (Nikitin, 2007). The experimental data confirmed the heat exchanger high performance. At the same time the numerical experiments performed using CFD FLUENT code [5] demonstrated the 10–15% accuracy of *Nu* number simulation and 20% accuracy of pressure drop factor simulation obtained for an MCHE with S-shaped fins. The difference obtained might be explained by the fact, that the inlet and outlet distributors were not simulated.

The direct way to understand the effect of the inlet and outlet distributors on the heat transfer and pressure drop characteristics of MCHE is to perform the detailed full-scale simulations using available computational fluid dynamics (CFD) code. CFD applications which simulate fluid flow in heat exchangers are based on the numerical solution of Reynolds time-averaged Navier-Stokes equations. The solution depends mainly on an appropriate geometrical model, mesh definition and the selection of a turbulence model.

## COMPUTATIONAL METHOD

## MCHE: design, computational model

A new MCHE, with S-shaped fins based on a sine curve, was proposed in a previous study. The experimental study confirmed the pressure drop is 4-5 times less than that of a conventional MCHE with zigzag fluid channels, while the degradation of heat transfer performance is moderate. The fluid channels are produced using chemical etching of a metal plate. Then the plates are stacked together in a double banking configuration (hot-cold-hot-hot-cold-hot-hot-cold...) and diffusion bonded under high-pressure and high-temperature conditions. Geometrical data and picture are shown in Table 1 and Fig.1 respectively.

Table 1 MCHE specifications.

| Parameter | Side | Value |
|---|---|---|
| Plate thickness, mm | Cold/Hot | 1.5 |
| Channel depth, mm | Cold/Hot | 0.94 |
| Channel width, mm | Cold/Hot | 1.31 |
| Fin/wall thickness, mm | Cold/Hot | 0.8 |
| Hydraulic diameter, mm | Cold/Hot | 1.09[a)] |
| Bending angle, ° | Cold/Hot | 76 |
| Pitch in *x*-direction /*y*-direction, mm | Cold/Hot | 7.565/3.426 |
| Number of plates | Cold | 4 |
| | Hot | 8 |
| Number of fluid channels | Cold | 44 |
| | Hot | 96 |
| MCHE dimensions H/W/D, mm | - | 745.2/76/29 |
| Heat transfer area, $m^2$ | Cold | 0.2559 |
| | Hot | 0.5099 |
| Free flow area, $m^2$ | Cold | $5.42 \times 10^{-5}$ |
| | Hot | $11.82 \times 10^{-5}$ |

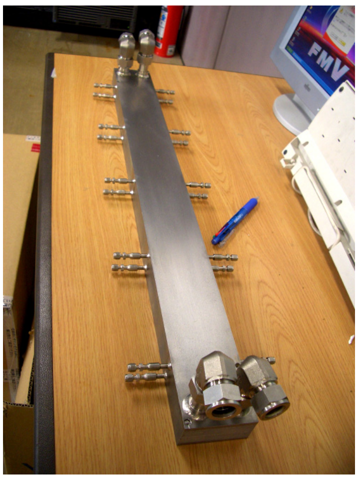

Fig. 1. Picture of MCHE with S-shaped fins.

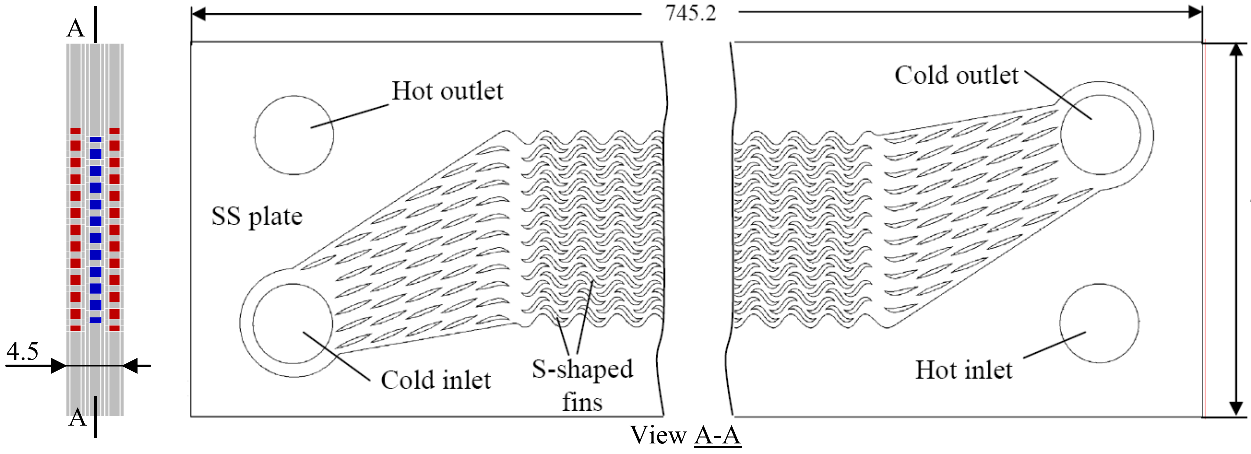


Fig. 2. Computational domain.

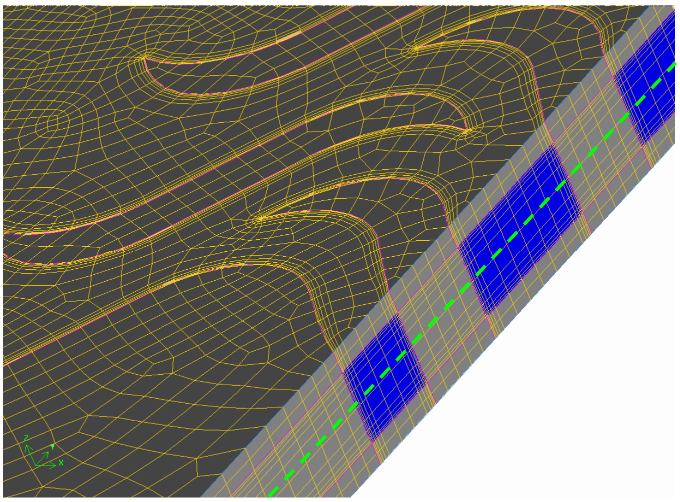

Fig. 3 Fragment of mesh of cold side plate. The dashed green line is used to plot a temperature profile.

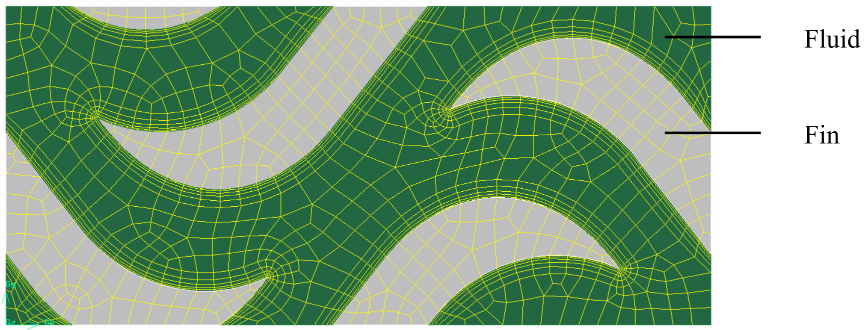


Fig.4 Mesh in *x-y* plane (3.462×7.256 mm).

The computational domain is shown in Fig. 2. The inlet cold side distributor is drawn in A-A view. The corresponding mesh in an enlarge scale is shown in Fig. 3. The zero-heat-flux boundary conditions were applied for the upper/bottom surfaces and side walls. The mass flow inlet conditions were used for the cold and hot fluid inlet. The initial cell number is as high as $4.8 \times 10^7$. The computational time using a single CPU is ca. 600 h (HP rx4640 workstation). The mesh size is chosen to be the maximal possible for the available memory size. The typical mesh in *x-y* plane is shown in Fig. 4. In *z*-direction the mesh in fluid region was constructed using the boundary layer with the following characteristics: the first row depth is 0.03 mm, the growth factor is 1.5. The mesh refining was not performed due to the available memory limitation.

**Turbulence model and mesh size**

The choice of turbulence model depends on considerations such as the physics encompassed in the flow, the level of accuracy required, the available computational resources, the amount of time available for the simulation, etc. Preliminary calculations of Weisbach experiment were done to check different turbulence models applicability.

The RNG model with enhanced wall treatment demonstrated the best agreement with the experimental data for tube bending angles up to 60° as shown in Fig. 5. The bending angle of the MCHE channels with S-shaped fins is 52°.

Then the RNG *k-ε* viscous model with enhanced near-wall treatment was applied in the simulation. When an initial solution was obtained, the grid was adapted based on $y^+$ values. A second-order discrimination scheme was used for momentum, energy, turbulence kinetic energy, and dissipation rate equations and SIMPLE pressure-velocity coupling.

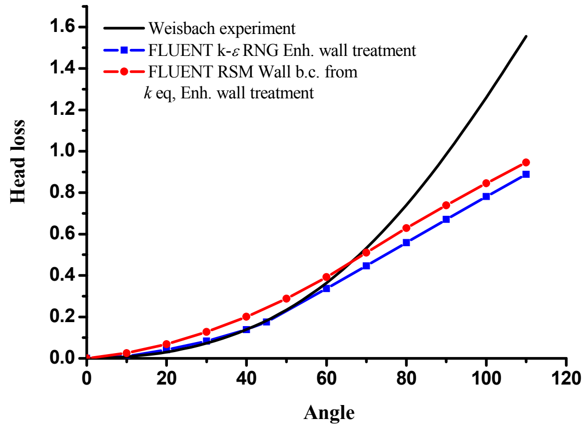


Fig.5. Head loss coefficient

**$CO_2$ property data base**

A $CO_2$ database was prepared using PROPATH libraries. The properties were calculated in 30 points for a specified temperature range, inlet pressure and expected pressure drop for both the hot and cold sides. The linear change of pressure with temperature was assumed. Because the pressure drop is rather small this assumption doesn't affect the accuracy of CFD calculations. The calculated thermophysical properties of hot side and cold side fluids are shown in Fig. 6 as a function of temperature.

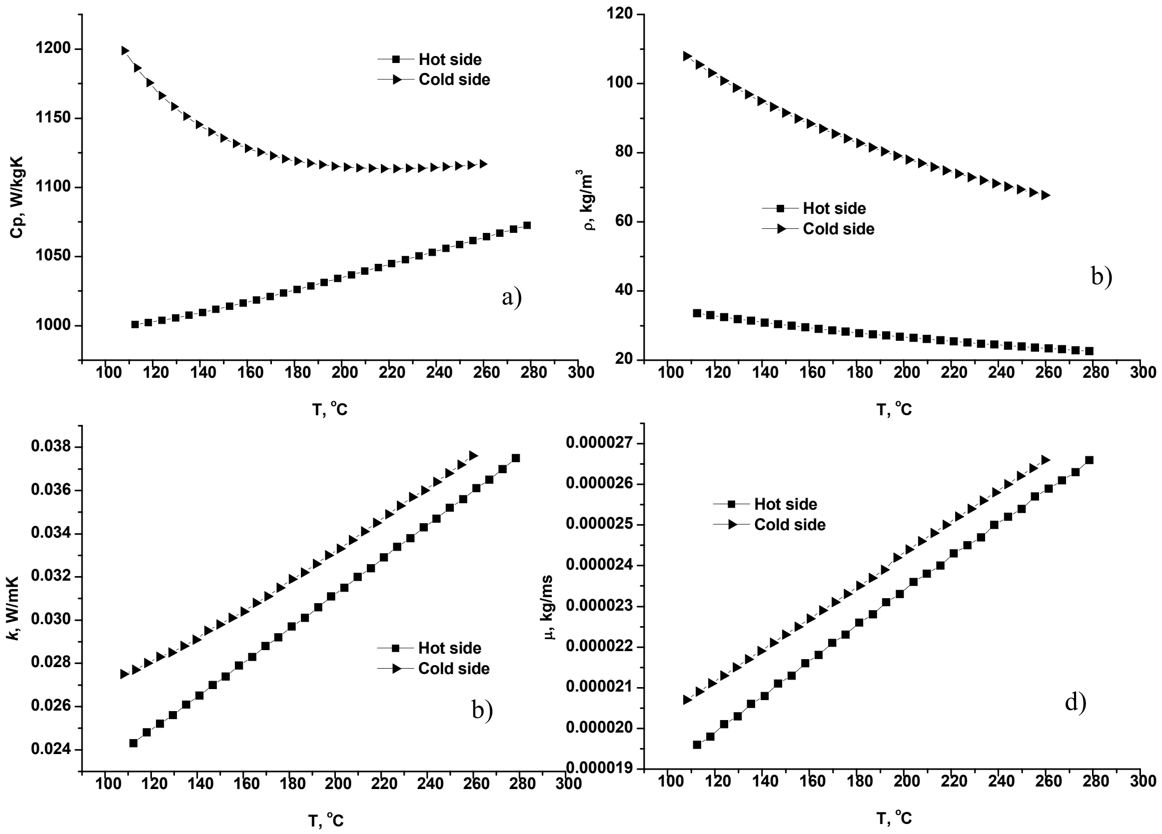


Fig. 6 Fluid thermophysical properties used in CFD simulations: a) specific heat, b) density, c) thermal conductivity, d) viscosity.

**Simulation conditions**

The available experimental data [1] were used to define the simulations conditions. An experimental facility was built in TIT to measure thermal-hydraulic parameters of supercritical $CO_2$ on the MCHE inlet and outlet under different operating conditions. The heat loss from the MCHE outer surface was fully compensated using strap heaters installed inside the insulator. The experiments were performed in a wide range of fluid inlet conditions which similar to actual operating conditions for recuperator of $SCO_2$ gas turbine cycle. The inlet temperatures of hot and cold sides were fixed at the level of 280 and 108°C respectively. The inlet pressure of hot side was varied in the range from 2.2 to 3.5 MPa. The inlet pressure and $CO_2$ flow rate are shown in Fig. 7. The conditions chosen for CFD simulation are marked by circles.

The inlet fluid parameters taken for CFD simulations are summarized in Table 2. Roughly speaking these conditions cover all the range of experimental conditions. The corresponding Re number range is from 3000 to 19100.

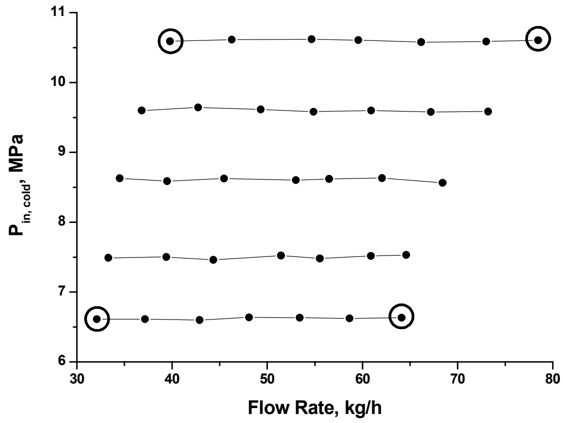


Fig.7 Inlet pressure and $CO_2$ flow rate.

Table 2. Experimental data.

| Case | 1 | | 2 | | 3 | | 4 | |
|---|---|---|---|---|---|---|---|---|
| Side | Hot | Cold | Hot | Cold | Hot | Cold | Hot | Cold |
| Tin, K | 551.59 | 381.06 | 552.21 | 380.84 | 551.82 | 380.71 | 552.29 | 380.95 |
| Tout, K | 385.58 | 532.68 | 388.35 | 530.66 | 383.06 | 523.45 | 385.25 | 522.13 |
| Pin, MPa | 2.334 | 6.610 | 2.311 | 6.631 | 3.617 | 10.589 | 3.580 | 10.606 |
| ΔP, kPa | 9.21 | 10.72 | 34.83 | 38.19 | 11.030 | 11.681 | 30.12 | 30.24 |
| G, kg/s | 0.008914 | | 0.01781 | | 0.011046 | | 0.021794 | |
| Q, W | 1529.43 | | 3014.43 | | 1974.86 | | 3852.34 | |

## RESULTS AND DISCUSSIONS

The results of CFD simulation was compared with the experimental data. The experimental facility, data reduction process and experimental data are described in details in Ref. 4. The experimental data are divided into two classes, integral characteristics and 3-D distributions. The integral parameters are the inlet and outlet temperatures, flow rate and corresponding heat load, pressure loss. Some other characteristics, for example an overall heat transfer coefficient, might be derived from integral characteristics. 3-D distributions include the temperature distributions, fluid velocity distributions, pressure fields etc.

**Integral characteristics**

Numerical results for the total heat transferred from hot to cold fluid, pressure drops as well as overall heat transfer coefficient are presented. The geometrical factor, *F*, is calculated from the heat balance equations. The most important integral parameters are given in Table 3. The number of heat exchanger plates in CFD simulations and consequently the flow rate is four times less comparing to those of the real MCHE that has been tested. Therefore, for comparison purpose, the heat load obtained in numerical simulations is multiplied by factor 4. The large difference in the pressure drop (up to 29%) might be explained by the difference between the cross-sectional area and shape of the real fluid channel and that which is used in the simulation (rectangular shape).

Table 3 Results of CFD simulation

| Case | 1 | 2 | 3 | 4 |
|---|---|---|---|---|
| Q, W | 1528.2(-0.02%)* | 3026.8(0.32%) | 1984.4(0.48%) | 3862.3(0.26%) |
| U, $W/m^2K$ | 251.52(-0.37%) | 410.38(4.38%) | 288.28(-11.32%) | 480.24(1.15%) |
| $\Delta P_{hot}$, kPa | 10.38(12.7%) | 36.65(5.2%) | 9297(-16.4%) | 40268(+33.7%) |
| $\Delta P_{cold}$, kPa | 13.83(29.0%) | 48.79(27.8%) | 11544(-0.7%) | 33049(+9.3%) |

* Deviation from the experimental data, e.g. $(Q_{CFD} - Q_{\exp})/Q_{\exp}$

**Geometrical factor**

The geometrical factor, $F_G$, is introduced to take into account the heat transfer degradation in non-counter flow parts of heat exchanger [2] in the following form

$$Q = UAF_G \Delta T_{\text{mean}} \quad (1)$$

Suppose one considered two heat exchangers, a reference counterflow exchanger and the exchanger in question. Each is to operate with the same Q, inlet fluid temperatures and flow rates. It then follows that $\Delta T_{mean}$ will be the same for the two heat exchangers and

$$F_G = \frac{A_{counterflow}}{A} \leq 1 \quad (2)$$

or

$$F_G = \frac{U}{U_{counterflow}} \leq 1 . \quad (3)$$

The overall heat transfer coefficient, *U*, was estimated from FLUENT calculations. The definition of the mean temperature difference of two fluids is taken from Ref [1]. For the counterflow part of MCHE the mass-weighted averaged temperature were used. The result of simulation for Case 1 is presented in Table4. The results for the cases 2-4 are similar.

Table 4. Geometrical factor data. Case 1

| MCHE part | U, W/m$^2$K | F |
|---|---|---|
| Whole | 255.3 | - |
| Counterflow (region 1-4 in Fig. 7) | 287.6 | 0.887 |

The obtained result means that the amplitude of Nusselt number correlations reported in Ref. 3, 4 should be increased by factor 1/0.887. It is important also that 6.3% of heat is transferred through the inlet/outlet distributor (the leftmost and rightmost zones in Fig. 8) while the respective heat transfer area is 9.0% of the total heat transfer area. At the same time the pressure drop in the inlet/outlet distributors is 6.5% for the hot side and 5.4% for the cold side. The obtained results indicated that the heat transfer rate and pressure drop is approximately 1.5 times less in the inlet/outlet distributors comparing to those in the cross-flow parts. Obviously the heat transfer rate may be increased by changing the shape/number of fins in the inlet/outlet distributor zones at the expense of increased pressure drop.

**3D distributions**

Twenty thermocouples of 0.5 mm ∅ were installed inside hot and cold fluid channels to measure the fluid temperatures of hot and cold sides during the experiments. Thermocouples channels may be seen in Fig. 1. The thermocouple positions are given in Fig 8. The thermocouple

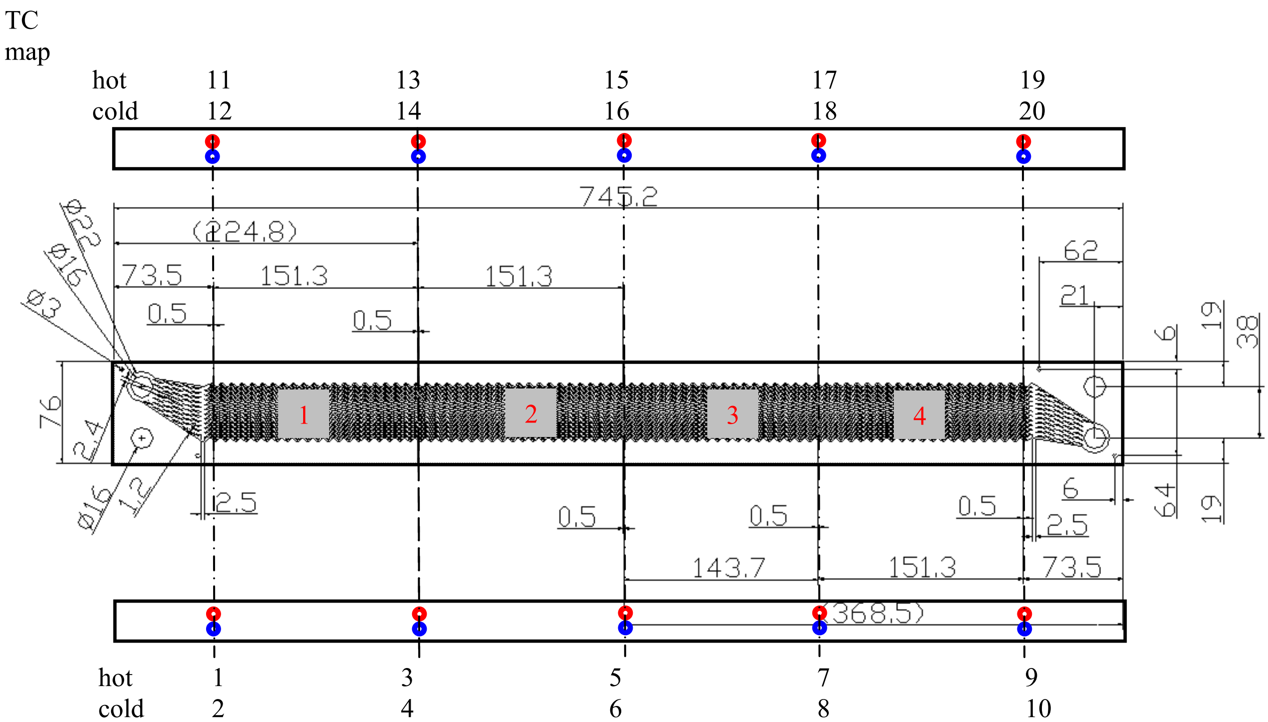


Fig. 8 Test section (hot plate) and TC map

The thermocouple temperatures near the inlet and outlet regions were compared with the simulation results. The corresponding temperature profiles and the experimental data are plotted in Fig. 9 and 10. The temperature is greatly varied along the cross-section of each fluid channel. The average fluid temperatures in the channels are also varied.

These two effects cause troubles for the temperature reconstruction using thermocouples data. In order to find the correct heat balance data the temperature measured by thermocouples must be corrected according to the real temperature profile which might be obtained by CFD analysis.

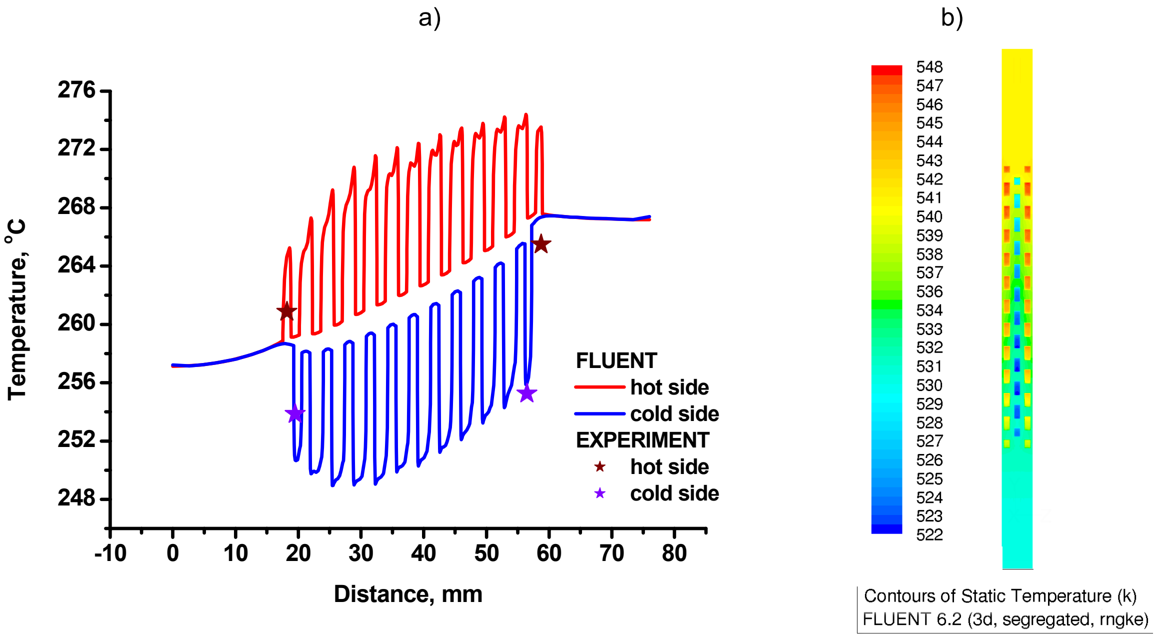


Fig.9 Temperature distribution obtained by a) CFD calculations and the experiment, and b) the corresponding contours of static temperatures,. The position is 73.5 mm from the right MCHE side in Fig.8.

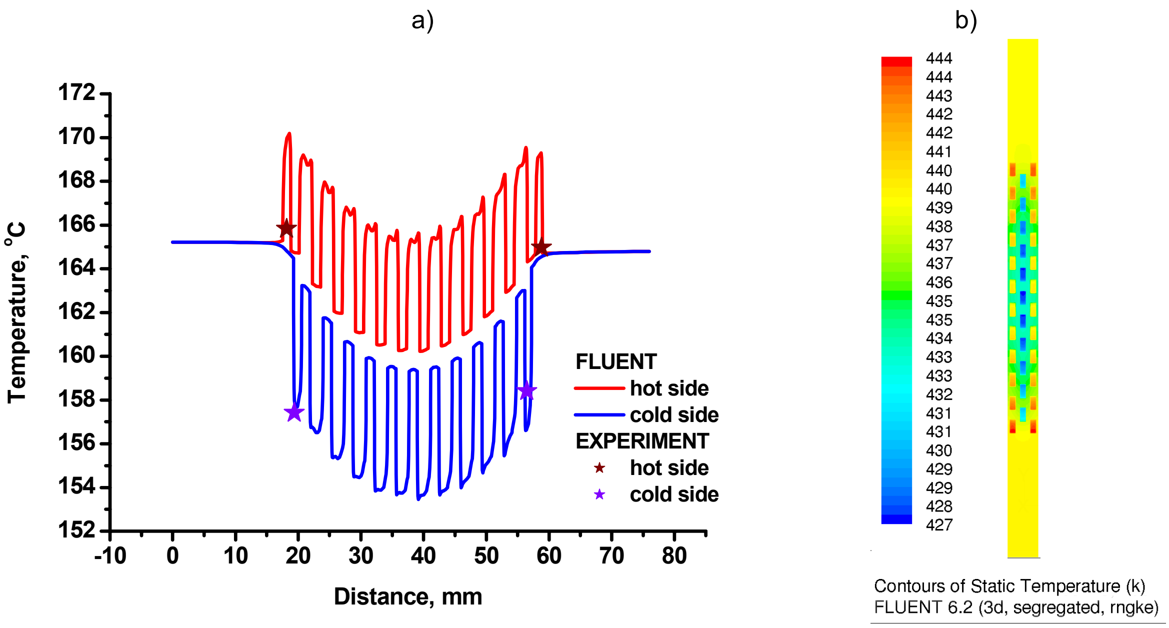


Fig. 10 Temperature distribution obtained by CFD calculations and in the experiment, a), and the corresponding contours of static temperatures, b). The position is 368.5 mm from the right MCHE side (Center) in Fig.8.

## CONCLUSIONS

Heat transfer and pressure drop characteristics of MCHE with fluid channels formed by S-shaped fins were calculated by CFD FLUENT code. Three central plates or ¼ part of heat exchanger were simulated. The simulation results were compared with the previously obtained experimental data.

The results of simulations are in a good agreement with the experimental data for the temperature distributions, heat load and overall heat transfer coefficient. The accuracy of overall heat transfer coefficient prediction is 11% that is within the experimental data uncertainty for the overall heat transfer coefficient. The pressure drop is overestimated by 5-30% which is higher than the experimental uncertainty for the pressure drop. The geometrical factor which is to be used in the experimental data treatment seems to be equal 0.89. The heat transfer rate and pressure drop is approximately 1.5 times less in the inlet/outlet distributors comparing to those in the cross-flow parts of MCHE.

## REFERENCES

1. Kato, Y., Nitawaki,T. and Muto,Y.(2004):"Medium temperature carbon dioxide gas turbine", *Nuclear Engineering and Design*, Vol.230, pp.195-207
2. Muto, Y., Nitawaki, T. and Kato, Y.(2003);" Comparative design study of carbon dioxide gas turbine for HTGR power plant", #3313 *Proc. of 2003 International Congress on Advanced Nuclear Power Plants (ICAPP'03)*, Cordova, Spain, May 4-7,
3. Tsuzuki, N. Kato, Y. and Ishizuka, T.( 2005):" High Performance Printed Circuit Heat Exchanger", *HEAT-SET2005,* France
4. Nikitin, K., Kato, Y. and Ishizuka, T.( 2007):" Experimental thermal-hydraulics comparison of microchannel heat exchangers with zigzag channels and S-shaped fins for gas turbine reactors", paper 10826 *ICONE-15*, Nagoya, Japan, April 22–26
5. FLUENT, Inc.( 2006):" Fluent 6.2 User's guide, Fluent Inc., Lebanon, NH.